Scalar scattering model of highly textured transparent conducting oxide

Chien-Chung Lin, Wei-Lin Liu, and Chi-Ying Hsieh

Citation: Journal of Applied Physics **109**, 014508 (2011); doi: 10.1063/1.3530684
View online: http://dx.doi.org/10.1063/1.3530684
View Table of Contents: http://scitation.aip.org/content/aip/journal/jap/109/1?ver=pdfcov
Published by the AIP Publishing

Scalar scattering model of highly textured transparent conducting oxide

Chien-Chung Lin,[a] Wei-Lin Liu, and Chi-Ying Hsieh
Institute of Photonic Systems, College of Photonics, National Chiao-Tung University, Tainan 71150, Taiwan

(Received 15 September 2010; accepted 19 November 2010; published online 13 January 2011)

Amorphous silicon solar cell is one of the most well developed solar energy solutions. In order to increase the energy conversion efficiency, light-trapping is necessary to the cell structure. Light trapping can be achieved by a textured transparent conducting oxide (TCO) layer and one of the critical factors of textured TCO is its haze value, which characterizes the scattering capability of the TCO. Recently several highly textured TCOs were presented with high haze at near IR region, where the haze of textured interfaces traditionally suffered from reduced scattering. However, suitable modeling is not established yet. In this work, we use scalar scattering theory and Kirchhoff approximation to solve haze value of complex surfaces analytically. Different from original Rayleigh scattering expression, this model illustrates intricacy between the surface roughness, correlation length, and the separation between different groups of height distributions. The resulting analytical formulation can be applied successfully not only in regular monotonically decaying spectral hazes but also various nonmonotonically shaped ones, meanwhile it retains important physical factors which can be useful for process evaluation. © *2011 American Institute of Physics*. [doi:10.1063/1.3530684]

I. INTRODUCTION

In recent years, hydrogenated amorphous silicon (a-Si:H) thin film solar cells have drawn much attention due to their low fabrication cost and tremendously flexible form. A generalized thin film solar cell of this kind (Fig. 1) is composed of thin absorbing layers (such as a-Si:H or polycrystalline Si), a transparent conducting oxide (TCO) layer, with top and bottom contact layers. While attempting to create a thin structure, the notion of increasing light absorption capabilities is an important concern. One key feature, called *light trapping*, aims at improving upon low absorption rates. Through reflection or scattering at interfaces or grain boundaries, light-trapping lengthens the traveling path of photon in the cells such that the absorption ability of the solar cells can be effectively increased. To achieve this goal, a technique involving corrugating interfaces between layers has been one of the most frequently applied methods; the corrugation can be either periodic or random.[1–3] In this scheme, the TCO layer plays an important role as it can be forged into different surface morphologies via different etching processes[2,4] and then act as a seeding layer so that the subsequent grown layers can duplicate this roughness. Processed and textured surfaces have shown advancements in terms of the quantum efficiency of solar cells.[5,6] The measure of TCO layer's scattering capability, or *haze value*, is thus a very important gauge of thin film solar cell's performance. The haze value is a ratio of scattered (diffused) light over the total reflection (or transmission).

The theoretical understanding of light scattering on a rough surface can be traced back to the late 1950s. Light scattering is a basis of remote-sensing, computer graphics, and advanced optics, all of which are as important in today's technological society as they were 60 years ago. In the seminal work by Davies and Porteus,[7,8] the researchers started from scalar scattering theory to derive the basic formula of a randomized rough surface. Later, in 1963, Beckmann and Spizzichino[9] published thorough analyses on the scattering of rough surfaces. All of these sources focused on the reflected waves by conducting rough surfaces. Recently, several papers also proposed numerical calculation routines of haze (or the angular distribution function of scattered light) based on Born-approximation,[10] the Fourier optics method,[11] phase perturbation theory,[13] and the Beckmann–Kirchhoff theory.[14] However, most of the research has emphasized on the rough surface with single Gaussian distribution of its height,[7–9,11,12] and no theoretical analyses on the scattering of complex surface have been performed.

In this paper, we are aiming to provide an approximate analytical solution of a highly textured TCO's haze value. This solution can be helpful toward determining the characteristics of a textured TCO quickly and without a complicated computer program. At the same time, the analytical solution retains key features which can affect the dispersion of haze, such as root-mean-square (rms) roughness, and can provide valuable information for a process evaluation of a TCO. This paper is organized as follows. First, we will re-

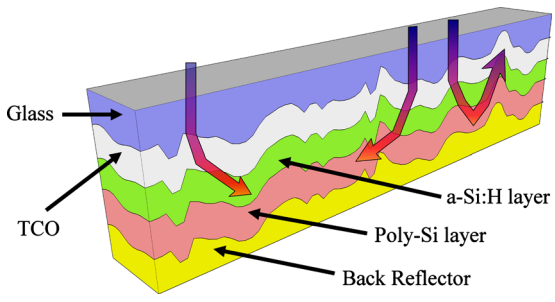

FIG. 1. (Color online) Schematic diagram of a general thin film solar cell with light trapping/scattering feature.

[a]Electronic mail: chienchunglin@faculty.nctu.edu.tw.

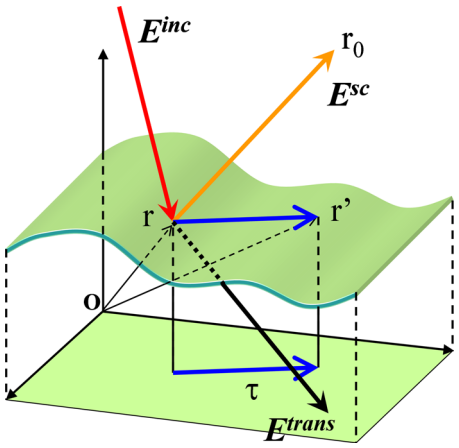

FIG. 2. (Color online) Schematic diagram of a diffracted radiation on rough surface.

view general scalar scattering theory using the Fresnel–Kirchhoff diffraction formula. The scalar theory of reflection has been well established but to apply similar assertions to transmission, the formulation requires some modification. Second, we will analyze the haze formula for regular rough surfaces with Guassian height distribution and highly textured surfaces which have not been previously theoretically examined. Finally, we will verify our theory with available experimental databased on this theory and a successful match to our model will be demonstrated.

II. DESCRIPTION OF RANDOM ROUGH SURFACES

Random rough surface cannot be described in any deterministic fashion (such as periodicity of structure) while still showing certain statistical properties of its physical form, like height or the shape of bumps and valleys on the surface. As shown in Fig. 2, a rough surface with an average height as the reference level undulates around this level. The probability, D(z), of being a specific height z at location x can be associated to a certain statistical distribution, i.e., Gaussian distribution. A randomized texture surface with Gaussian height distribution can be characterized by two important features: its rms roughness, σ, and the correlation length, a_{corr}. Both of these can be found from direct atomic force microscopic (AFM) measurements of the surface. In general, the probability density function D(z) of the Gaussian surface profile z(x) with a mean value of height, μ, can be expressed as:[8]

$$D(z) = \frac{1}{\sqrt{2\pi\sigma^2}} e^{-(z-\mu)^2/2\sigma^2}. \quad (1)$$

While we can always assume or set the mean value of distribution as reference ($\mu=0$), it is the rms roughness, or the spread of the distribution that matters. The rms roughness can be defined as:

$$\sigma^2 = \langle z(x)^2 \rangle - \langle z(x) \rangle^2, \quad (2)$$

where z(x) is the height of the surface and $\langle\ \rangle$ shows the averaged value.

The other important coefficient is the correlation length of the texture surface defined by its autocorrelation function (ACF, sometimes called *autocovariance function*). The ACF of a random rough surface can be treated as:[13,15]

$$C(\tau) = \lim_{L\to\infty} \frac{1}{2L\sigma^2} \int_{-L}^{L} z(x)z(x+\tau)dx, \quad (3)$$

where L is usually the range of surface scanning and σ is the rms roughness of the surface. From Eq. (3), we can link the rms roughness to this ACF at $\tau=0$: $C(0)=\sigma^2$, if we set the average height of surface to zero. The correlation length, a_{corr}, can be defined as:[8]

$$a_{corr}^2 = \frac{2}{\sigma^2} \int_0^{\infty} \tau C(\tau) d\tau. \quad (4)$$

There are two types of $C(\tau)$ that are often observed: one is the Gaussian type, and the other is the exponential decaying type.[13,15] $C(\tau)$ should be largely determined by the actual lateral correlation between points on the surface, so it will be location-sensitive if the surface is not isotropic. In this paper, we assume that all surfaces we deal with are isotropic.

III. SCALAR SCATTERING THEORY FOR RANDOM ROUGH SURFACES

In the past, the reflective scattering formulation of a rough and conducting surface has been well-established, both numerically and analytically.[8,9,16,17] Most of the theoretical results were derived from Maxwell or Helmholtz equation, and then from either Green's theorem or the Fresnel–Kirchhoff diffraction formula[8,16,17] to handle the reflective radiation.

The diffracted waves can be further categorized into two parts: the specular part and the diffused part. They are sometimes called coherent and incoherent components, respectively. When incidental electromagnetic waves impinge on the surface, if the surface is mirrorlike and flat, all the reflected and transmitted rays follow geometrical optics and Snell's law. These are referred to as the specular directions of reflection and transmission. However, when the surface is wrinkled, there are certain percentages of electromagnetic waves reflected or transmitted into other directions due to different microscale or nanoscale surface orientation. From a macroscale viewpoint, these off-specular components are categorized as diffused or incoherent components.

The coherent reflectance, without considering multiple reflection or shadowing effects, has been derived previously:[7,8]

$$R_C = R_0 \cos^2\psi \left| \int_{-\infty}^{\infty} D(z) \exp\left[-\frac{4\pi i z}{\lambda} \cos\psi \right] dz \right|^2, \quad (5)$$

where R_0 is the reflectance at normal incidence when the surface approaches perfect flatness, D(z) is the density function of surface height, and ψ is the incident angle. This expression is derived from the regular Fresnel–Kirchhoff diffraction formula.[8] If the incoming radiation is normal to the surface, then $\psi=0$ and the above equation becomes:

$$R_C = R_0 \left| \int_{-\infty}^{\infty} D(z) \exp\left[-\frac{4\pi i z}{\lambda} \right] dz \right|^2. \quad (6)$$

On the incoherent reflectance, we can follow the same derivation and it can be shown as:[8]

$$\begin{aligned} R_{incoherence} &= R_{diffused} \\ &= \int\int\int p(\tau) \exp[-i\vec{k}_d \cdot \vec{\tau}] D(z) \\ &\quad \times \left(1 - \int D(z') \exp[-4\pi i (z-z')/\lambda] dz' \right) \\ &\quad \times dz d\tau d\Omega \\ &= R_0 \int\int p(\tau) \exp[-i\vec{k}_d \cdot \vec{\tau}] \left(1 - \frac{R_C}{R_0} \right) d\tau d\Omega \\ &\approx R_0 \left(1 - \frac{R_C}{R_0} \right) (1 - \exp[-(\pi a_{corr} \alpha/\lambda)^2]), \end{aligned} \quad (7)$$

where k_d is the wave vector of the diffracted wave, τ is the projected x-y plane vector between two points on the interface (r and r′ shown in Fig. 2), Ω is the solid angle, and α is the semivertex angle of the acceptance cone. The function $p(\tau)$ introduced here is the probability that two random points on the rough surface with a distance τ apart will lie at an equal level;[8] this can be related to ACF by: $C(\tau) = \sigma^2 p(\tau)$. In this equation, we have assumed: (a) the rough surface is isotropic, such that the joint density of height distribution depends on the magnitude of τ but not its direction; (b) normal incident; and (c) a small acceptance angle such that the z-axis component of k vector can be approximated by $4\pi/\lambda$.[8]

Next, we will carry out the analysis of the transmission case. Similar to reflection mode, electromagnetic waves pass through the air-TCO interface with the assumption that there are no multiple scattering processes. The transmitted field can be simply expressed as the combination of the transmission coefficient T_0 and the incident field: $E^{trans} = T_0 E^{inc}$, and E^{trans} and E^{inc} are the transmitted and incident electromagnetic fields, respectively. Based on Green's theorem and Helmholtz equations[16,17] and the aforementioned assumption, we can further assert that the coherent transmittance can be written as (see Appendix for details):

$$T_C = T_0 \left| \int_{-\infty}^{\infty} D(z) \exp\left[-\frac{2\pi i z}{\lambda} (n-1) \right] dz \right|^2, \quad (8)$$

where n_{TCO} is the refractive index of the TCO material and where the radiation is at a normal angle.

Based on the methodology in Porteus's paper[8] and explanations in Appendix, we could then follow a similar procedure of reflectance and rewrite the diffused transmission term (incoherent transmission) as:

$$\begin{aligned} T_{incoherent} &= T_{diffused} \\ &= T_0 \int\int\int\int [D(z)\delta(z-z')p(s) \\ &\quad - D(z)D(z')p(s)] \\ &\quad \times \exp\left[-\frac{i2\pi}{\lambda}(n-1)(z-z') - i\vec{k}_d \cdot \vec{s} \right] \\ &\quad \times dz dz' ds d\Omega \\ &= T_0 \int\int p(\tau) \exp[-i\vec{k}_d \cdot \vec{\tau}] \left(1 - \frac{T_C}{T_0} \right) d\tau d\Omega \\ &\approx T_0 \left(1 - \frac{T_C}{T_0} \right) (1 - \exp[-(\pi a_{corr} \alpha/\lambda)^2]). \end{aligned} \quad (9)$$

This equation gives us a simple way to calculate the haze value in Sec. IV.

In summary, we derive the expressions of coherent and incoherent transmittances from scalar scattering theory. In addition, we found that the difference between reflection and transmission, under the assumption of a single scattering event at normal incidence, is only in the phase of Eqs. (6) and (8), and that this result complies with recent analyses:[10,13,16,18]

$$\begin{aligned} \phi_{reflection} &= 4\pi n_{air}/\lambda, \\ \phi_{transmission} &= 2\pi[n_{TCO}(\lambda) - n_{air}]/\lambda, \end{aligned} \quad (10)$$

where n_{air} and $n_{TCO}(\lambda)$ are the refractive indices of the air and TCO layers, respectively. The coherent and incoherent components [Eqs. (6)–(9)] comprise the foundation of haze calculation in Sec. IV.

IV. HAZE VALUE FOR SINGLE AND DUAL GAUSSIAN DISTRIBUTIONS

As we have mentioned, the haze value of a medium is defined by: (diffused component) /(specular+diffused components) and this can be applied to both reflection and transmission. In the past, the ordinary transmission haze for a regular textured TCO follows the simplified Rayleigh scattering formula:[12,19,20]

$$H_T = 1 - \exp\left[-\left(\frac{2\pi\sigma C(n_0 \cos\theta_0 - n_1 \cos\theta_1)}{\lambda} \right)^2 \right], \quad (11)$$

where σ, λ, n_0, n_1, θ_0, and θ_1 are the rms roughness, wavelength, refractive index of incident material, and transmitted material, angles of incidence, and transmission, respectively. However, the above formula is based on a single Gaussian distribution and did not consider lateral correlation entirely. When the texture distribution becomes complicated, these equations are not sufficiently accurate. To fit the measured haze properly, researchers have often resorted to different adjustments of the above formula,[12,19,20] for example, to change the exponent from 2 to 3:

$$H_T = 1 - \exp[-(4\pi\sigma C|\Delta n|/\lambda)^3], \quad (12)$$

where C is a fitting parameter and Δn is the refractive index difference between incident and transmission media. Even

though this modification delivered a satisfactory fit, it failed to obtain justification in terms of regular scattering theory.

On the other hand, Eqs. (6)–(9) are based on scalar scattering theory with proper assumptions and these expressions can be directly applied to haze value calculation. For a textured TCO layer, if the height distribution of the surface has Gaussian distribution, we can assume ACF following Gaussian distribution: $ACF=\sigma^2 p(\tau)=\sigma^2 \exp[-\tau^2/a_{corr}^2]$, where a_{corr} is the correlation length and σ is the rms roughness. The reflection haze[8] can be found directly from Eqs. (6) and (7):

$$H_R = \frac{R_{diffused}}{R_{total}} = \frac{(1-e^{-(4\pi\sigma/\lambda)^2})(1-e^{-(\pi a_{corr}\alpha/\lambda)^2})}{1-e^{-(\pi a_{corr}\alpha/\lambda)^2}(1-e^{-(4\pi\sigma/\lambda)^2})}, \quad (13)$$

where a_{corr} is the correlation length defined by ACF and α is the semivertex angle of the cone of acceptance.

Apply Eqs. (8) and (9), substitute ACF and D(z) in Eq. (9) and deduct the diffused transmission coefficient H_T as:

$$H_T = \frac{T_{diffused}}{T_{total}} = \frac{(1-e^{-(2\pi\sigma/\lambda)^2(n-1)^2})(1-e^{-(\pi a\alpha/\lambda)^2})}{1-e^{-(\pi a\alpha/\lambda)^2}(1-e^{-(2\pi\sigma/\lambda)^2(n-1)^2})}. \quad (14)$$

Equations (13) and (14) are more complex than their predecessors, Eq. (11) or Eq. (12), and the lateral (or planar) correlation between points on the surface is considered in the $\exp[-(\pi a_{corr}\alpha/\lambda)^2]$ term, which should complete the whole picture.

Next, we turn our attention to a more complicated case. From published results,[21,22] the surface of W-type TCO (or HU TCO) clearly contains at least two different types of height distribution. We can fit the AFM measured results with two different distributions and adjust their peak ratios. The corresponding density function of the surface height will become:

$$D(z) = Ae^{-(z-\mu_1)^2/2\sigma_1^2} + Be^{-(z-\mu_2)^2/2\sigma_2^2}, \quad (15)$$

where A and B are two constants to be found among AFM scan data and the coefficients, σ_i, μ_i, (i=1 or 2), represent the rms roughness and the mean of individual distribution, respectively. This new D(z) can be substituted into the original equations and elicit the coherent and incoherent reflectance as:

$$R_C = R_0\left\{\sigma_1^2A^2\exp\left[-\left(\frac{4\pi\sigma_1}{\lambda}\right)^2\right] + \sigma_2^2B^2\exp\left[-\left(\frac{4\pi\sigma_2}{\lambda}\right)^2\right] + 2\sigma_1\sigma_2AB\exp\left[-\left(\frac{\pi\sqrt{8(\sigma_1^2+\sigma_2^2)}}{\lambda}\right)^2\right]\times\cos\left(\frac{4\pi}{\lambda}(\mu_1-\mu_2)\right)\right\}, \quad (16)$$

$$R_{diffused} = R_0\left\{1-\frac{R_C}{R_0}\right\}\times\left(1-\exp\left[-\left(\frac{\pi a_{corr}\alpha}{\lambda}\right)^2\right]\right). \quad (17)$$

Similarly, the corresponding coherent transmission coefficient should be written as:

$$T_C = T_0\left\{\sigma_1^2A^2\exp\left[-\left(\frac{2\pi\sigma_1}{\lambda}(n-1)\right)^2\right] + \sigma_2^2B^2\exp\left[-\left(\frac{2\pi\sigma_2}{\lambda}(n-1)\right)^2\right] + 2\sigma_1\sigma_2AB\exp\left[-\left(\frac{\pi\sqrt{2(\sigma_1^2+\sigma_2^2)}}{\lambda}(n-1)\right)^2\right]\times\cos\left(\frac{2\pi}{\lambda}(n-1)(\mu_1-\mu_2)\right)\right\}, \quad (18)$$

where n is the refractive index of the medium. Following the previous derivation, the incoherent transmission coefficient is written as:

$$T_{diffused} = T_0\left\{1-\frac{T_C}{T_0}\right\}\times\left(1-\exp\left[-\left(\frac{\pi a_{corr}\alpha}{\lambda}\right)^2\right]\right). \quad (19)$$

The transmission haze can then be calculated according to the definition. As we can expect, since the joint density distribution is a linear combination of individual Gaussians, the final incoherent transmission is embedded in the same format of single-Gaussian transmittance but also with a coupling term due to the overall integration process.

V. COMPARISON TO EXPERIMENTAL RESULTS

So far, we have dealt with the formulation for the haze value of surfaces with either single Gaussian or dual Gaussian distributions. Next, we will focus on how well these equations fit with experimental results. Numerous experimental results of haze have been published[2,20,22–24] and we will use them to validate our formula. In general, the autocorrelation length (a_{corr}) can be extracted from AFM measurements by Eq. (4) or in the case of Gaussian ACF, we can calculate the autocorrelation length by fitting the ACF and extracting a_{corr} accordingly. The angle of acceptance, α, can then be estimated after a_{corr} is known by comparing haze values with Eqs. (13) and (14) or Eqs. (17)–(19). Another way to estimate the angle of acceptance is directly from the measurement apparatus. Usually, each measurement setup has its own source-receiver combination and, thus, the definition might be different case by case. Using accepted standards, e.g., ASTM D1003-95, we can define the semivertex acceptance angle as the angle between the perpendicular line through the center of the specimen and the line from the specimen's center toward the perimeter of the entrance pupil of the photodetector.[10] However, the autocorrelation length and angle of acceptance in our formula usually cannot be found from published results and will be treated as fitting parameters in our calculations.

A. Reflection haze

Reflection haze can be regarded as the stepping stone toward verifying the theory as there is only surface morphology concerning the scattering event. The fine conducting metal surfaces, whose rms roughness was usually much smaller than the incident wavelength ($\sigma/\lambda \ll 1$), were among

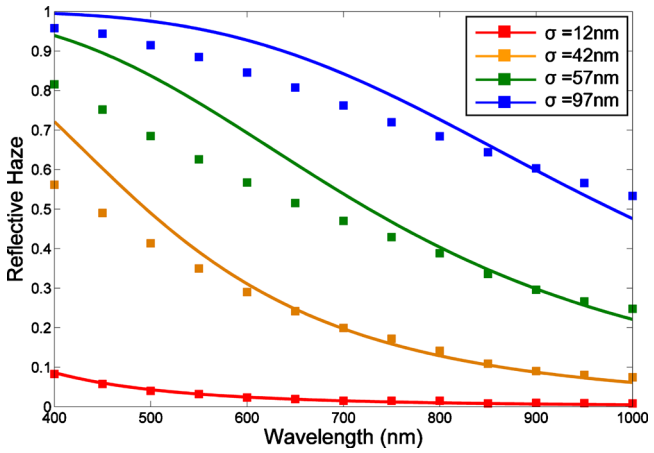

FIG. 3. (Color online) Reflective haze calculation and comparison to experimental results from Krc *et al.* (Ref. 5).

the first samples analyzed;[8,25] the haze can be treated using classical equations, i.e., Eq. (11). As for transparent surfaces with an rms roughness comparable to its wavelength, as with modern TCO structures, there have been several papers reporting measured reflective haze values.[23,24] Applying our formula in Eq. (13), we can see different degrees of fit to experimental results in Fig. 3. From the presented plot, the smooth surfaces (small σ) match very well while the rough surfaces (big σ) do not comply with our theory at shorter wavelengths. The reason for this could be such that the reflective haze in the data was taken from a TCO surface topped with a thin layer of conducting metal (for example, Ag), and while the scalar theory works fine for small σ/λ ratios, it will fail for a surface with a larger rms roughness due to shadowing and multiple reflection.[17,26] However, for transmission mode and dielectric interfaces, the scalar theory can be applied to a much wider range,[17,26] Another possibility lies in changing the ACF when the surface is rough, from a Gaussian-type to an exponentially decay-type through a non-conformal coating of thin metal layer.

B. Transmission haze

Transmission haze bears more importance nowadays since we need to maximize it in the context of solar cells.

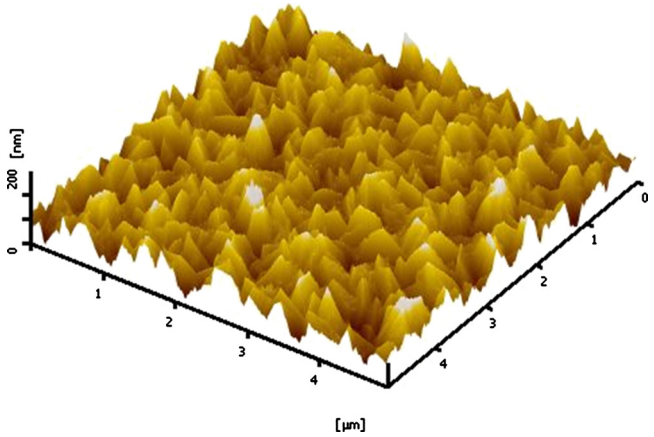

FIG. 4. (Color online) Two-dimensional AFM scanning of an Asahi U-type TCO surface.

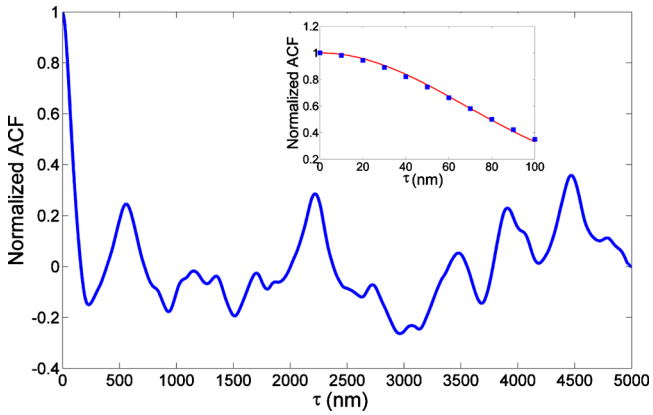

FIG. 5. (Color online) ACF of the Asahi U-type and the inset plot is the enlarged portion close to $\tau=0$ to illustrate the Gaussian fitting.

The Asahi U-type glass has been shown in several papers as the benchmark with which to evaluate the haze value of other TCOs and, initially, we will check our theory against it. Figure 4 shows the AFM scanned image of a regular Asahi U-type glass. Obtaining a cross-section profile from Fig. 4, we can calculate the rms roughness and correlation length of this textured surface.

Figure 5 shows the calculated ACF. The measured data points strongly suggest that the ACF of an Asahi U-type glass presents a Gaussian-like curve (inset plot of Fig. 5). The correlation length of this surface can then be determined as the variance of this curve. We picked 40 different locations from the scanned surface and calculated their corresponding correlation length values. Among these cross-sections, the average correlation length is 107 nm and the rms roughness is 38 nm. As for the refractive index of the TCO, we use the measured results and fitting parameters in the paper from Rakhshani, *et al.*,[27] in which they handled free electron dispersion in infrared regions with different expressions; agreement with experiment is very good. Using the above information, and an estimated acceptance angle of 0.48 rad, we further calculated our theoretical haze values and compared them to measured data, shown in Fig. 6.

Next, we will apply our theory to other published haze data pertaining to TCO surfaces with single Gaussian height distributions.[22] By applying Eq. (14), we can obtain a much

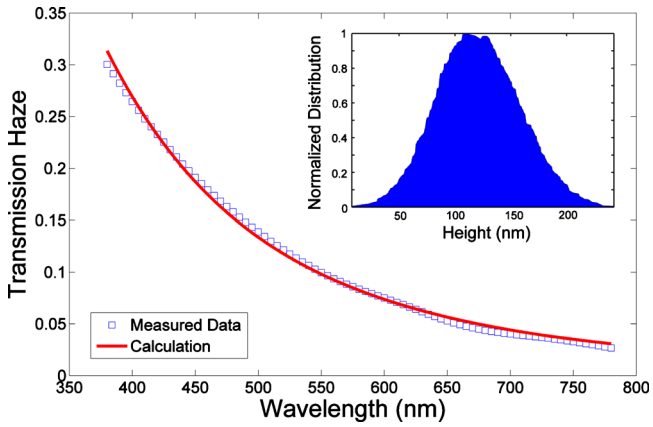

FIG. 6. (Color online) Transmission haze of a standard Asahi U-type TCO, and the inset is it surface height distribution function.

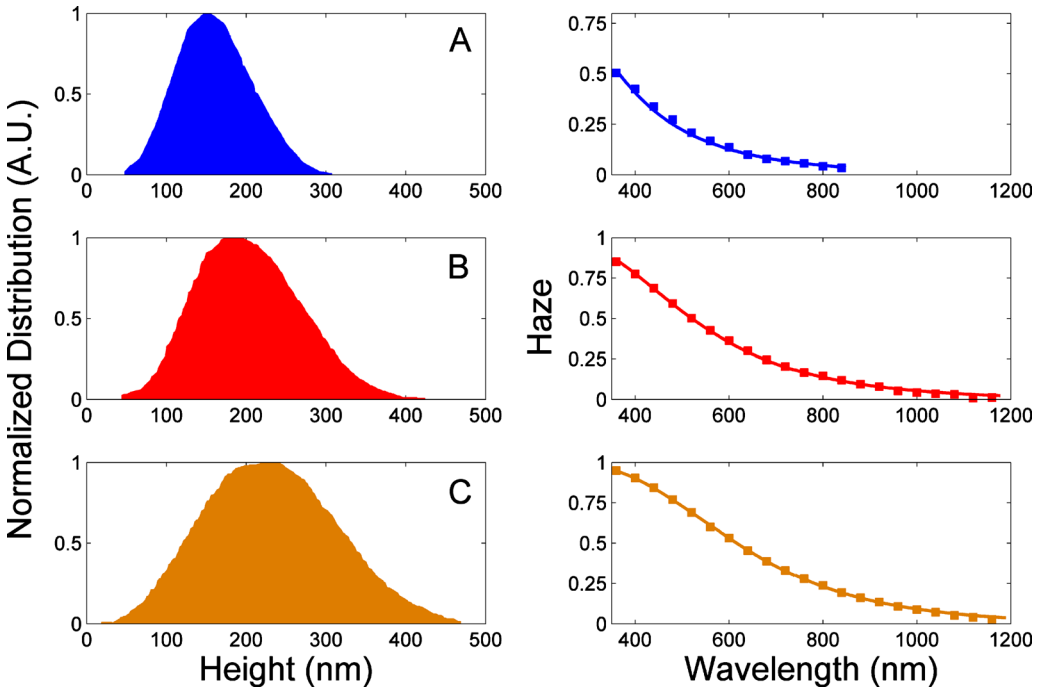

FIG. 7. (Color online) The surface with single Gaussian distributed height: left: surface height distribution from AFM; right: haze value calculated by our model (lines) and experimental data (squares) from Cording *et al.* (Ref. 22).

better fit to the experimental data. In Fig. 7, we demonstrate both the corresponding surface height distribution and transmission haze next to one another, while Table I summarizes the parameters we used in calculation. The rms roughness values are estimated from AFM scanned data on the left of Fig. 7, and the product of the autocorrelation length and the acceptance angle is treated as a fitting parameter.

A more challenging task is to extend this model to a more complicated surface, such as Asahi W-type TCO,[2,22] whose haze shape could not be calculated using Eq. (14). The double-peak height distribution (as shown in Fig. 8) gives another kind of spectral haze—a nonmonotonic, partially-cubiclike function. This feature largely comes from the coupling term in Eq. (19), and is related to the separation of the two distribution peaks. Our model can be successfully applied to accommodate these variations, as shown in Fig. 8. The rms roughness and peak value of individual height distribution are acquired from AFM data and are listed in Table II. During the fitting/calculation, we could see that the correlation length becomes very long, which tracks closely with a potential real situation. As we could see in Fig. 8, the calculated results using surface statistics as inputs can fit the actual haze very well. The slight deviation at longer wavelengths could come from our refractive index model's calculation.

TABLE I. Parameters for calculation in Fig. 7.

TCO surfaces	AFM σ (nm)	$a_{corr} \times \alpha$ (fitted)
A	47	59.3
B	67	87.4
C	87	96.4

C. Discussion

Several concerns regarding to the scalar model in this paper are discussed in this section and we hope this could be put forward as the first step toward solving a more complex surface scattering problem in the future. For surfaces with a mechanical polishing finish or one that uses a chemical process, many previous reports have showed that their height distributions are close to Gaussian statistics[11,28] and that the best way to verify this claim is to measure the surface profile using AFM. However, the current trend of TCO development is clearly steering toward more complicated surfaces, such as dual-Gaussian or even non-Gaussian. The model we develop here can be extended to multiple Gaussian-distributed surfaces as long as they are linearly combined. The majority of the derivation will be the same but the complexity of analytical equations [Eqs. (17)–(19)] will be greatly increased. On the other hand, if the height distribution is totally non-Gaussian, Eqs. (17)–(19) are not suitable for this case, then numerical integration of Eqs. (5)–(8) becomes necessary.

The validity of the scalar scattering model, together with Kirchhoff approximation (KA), is another relevant issue in the context of this analysis. The application of ray optics, Snell's law, and Fresnel equations rely on the surface feature size being much larger than the incident wavelength. It does not hold well in theory when the autocorrelation length of the surface is less than the incident wavelength and the surface is perfectly conducting.[29,30] From previous derivation[29,31] in the reflection mode, the ratio of surface roughness to autocorrelation length has to be small enough to allow the error to be less than 1% when the feature size is less than the incident wavelength. Moreover, as the incident angle varies, the accuracy of the model is reduced significantly.[31] As it has been pointed out, shadowing and

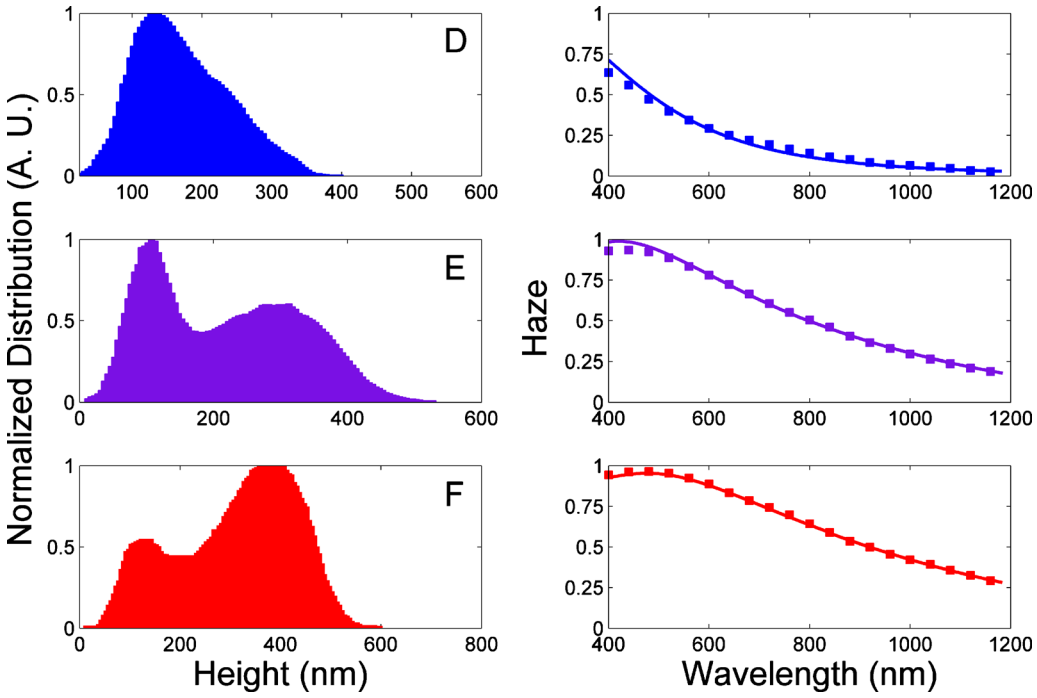

FIG. 8. (Color online) The surface with dual Gaussian distributed height: left: surface height distribution from AFM; right: haze value calculated by our model (lines) and experimental data (squares) from Cording *et al.* (Ref. 22).

backscattering both contribute non-traditional components which cause the traditional analysis to fail.[29,30] However, both effects are much weaker in the case of dielectric interfaces. From the numerical simulation presented by Sánchez-Gil and Nieto-Vesperinas,[17] the KA in dielectric transmission can hold much better than perfect conducting case at a zero incident angle. To better analyze this problem, we use the formula proposed in Ref. 29 and calculate how fast the KA deviates from the unitary condition when the feature size shrinks below incident wavelength. In addition, it is notable that this formula is based on conducting surfaces. Figure 9 shows the result of calculation at normal incidence. The limit of the plot signifies the applicable range of a_{corr}/λ and σ/a_{corr} in our TCO surfaces. As it can be seen, the worst error which our model is subject to is around 10% *in conducting surfaces*; however, this will be greatly reduced for transmission cases of dielectric interfaces.[17] So, we can assert that our scalar model can accurately describe a situation with less than 10% error and, in most cases, less than 2% error of the applicable wavelength regime.

VI. CONCLUSION

In conclusion, we have developed a semi-empirical model for a highly textured TCO diffused transmission coefficient. The analytical formula is based on scalar scattering theory and KA. We also identify important surface parameters of a TCO and their connection to the haze value. Through these findings, it is possible to predict any complex surface's haze value with only the surface profile scanned. A good match between experimental data and our calculations bolsters the validity of this assertion. Further modification of the method should be carried out to improve the accuracy of this useful analytical model.

TABLE II. Parameters for calculation in Fig. 8.

TCO surfaces	Peak separation (nm)	AFM σ_1 (nm)	AFM σ_2 (nm)	$a_{corr} \times \alpha$
D	96	56.6	41.7	199.6
E	180	91.9	33.8	323.3
F	255	84.2	55. 6	515.7

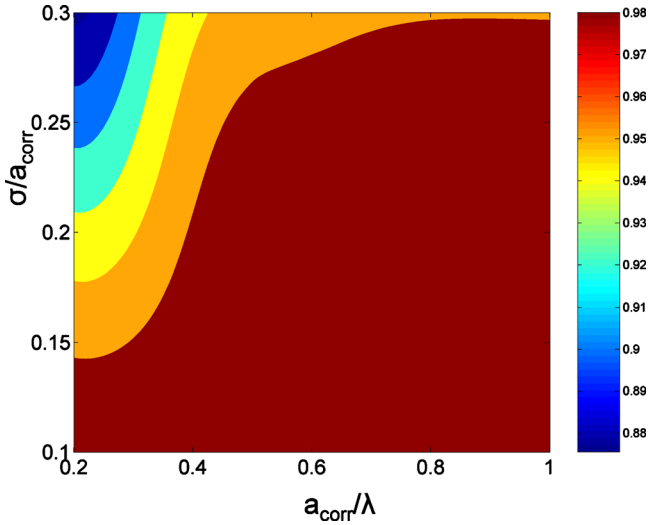

FIG. 9. (Color online) The plots of σ/a_{corr} vs a_{corr}/λ in perfect conducting surfaces at normal incidence. The colored zones mark the boundary of the error of the KA.

ACKNOWLEDGMENTS

The authors would like to thank Chi-Mei Energy Inc., for its support through research funding and technical discussion and C.-C. Lin would like to thank the National Chiao-Tung University of Taiwan for grant support. This work is partially supported by the National Science Council of ROC (Taiwan) Project No. NSC-99-2221-E-009-052-MY3.

APPENDIX: TRANSMISSION IN SCALAR THEORY

In this section, we would like to introduce our modification of the scalar theory for transmission. The following expressions are derived based on the assumption of no multiple scattering processes at the surface.

First, let us start from a reflection case. Refer to Fig. 2. We denote r_0 as a point in the medium of interest and r is the point on the rough surface. In regular scalar scatter theory, the reflective electromagnetic waves can be expressed as:[16,17]

$$E^{sc} = \frac{1}{4\pi}\int_{surface}\left(E^{total}\frac{\partial G}{\partial n} - \frac{\partial E^{total}}{\partial n}G\right)dS, \tag{A1}$$

where G is the Green function and can be written as: $\exp(in_1k|r-r_0|)/4\pi|r-r_0|$ and E^{total} is the total field (incident+scattered). In the KA, this total field can be further reduced to:[16,17]

$$E^{total} = E^{inc} + E^{sc} = (1+R_0)E^{inc}, \tag{A2}$$

where R_0 is the Fresnel coefficient. Furthermore, the derivative of the total field can also be reduced to:

$$\frac{\partial E^{total}}{\partial n} = i(1-R_0)(\vec{k}_{inc}\cdot\vec{n})E^{inc}, \tag{A3}$$

where $\vec{n}$ is the local outward normal vector. The final expression of reflection under the KA becomes:

$$E^{sc} = \frac{1}{4\pi}\int_{surface}\left[(1+R_0)\frac{\partial G}{\partial n} - i(1-R_0)(\vec{k}_{inc}\cdot\vec{n})G\right]E^{inc}dS. \tag{A4}$$

Similarly, the transmission formula can be written as:[16,17]

$$E^{sc} = \frac{1}{4\pi}\int_{surface}\left(E^{sc}\frac{\partial G}{\partial n} - \frac{\partial E^{sc}}{\partial n}G\right)dS. \tag{A5}$$

In this equation, the Green function is $\exp(in_2k|r-r_0|)/4\pi|r-r_0|$ now, as the refractive index is different. Meanwhile, the scattering field is $E^{sc}=E^{trans}=T_0\times E^{inc}$ because there is no other source on the other side of medium, and T_0 is the transmission coefficient. The derivative of the field is:

$$\frac{\partial E^{sc}}{\partial n} = iT_0(\vec{k}_t\cdot\vec{n})E^{inc}, \tag{A6}$$

where k_t is the wave vector of the transmitted light. So, we can treat the transmission as:

$$E^{sc} = \frac{1}{4\pi}\int_{surface}\left[T_0\frac{\partial G}{\partial n} - iT_0(\vec{k}_t\cdot\vec{n})G\right]E^{inc}dS. \tag{A7}$$

Comparing Eq. (A4)–(A7), we observe a certain similarity among scatter fields of reflection and transmission. To probe further, these equations lead to detailed angular dependent functions. If we limit ourselves to normal incidence and coherent component, many terms related to inclination and azimuth angles will be dropped out and the coherent reflection and transmission are truly different only in phase:[16]

$$I^{sc}|_{coherent} \propto \langle|E^{sc}(\theta=0)|^2\rangle = \begin{cases} R_0\int \exp[-i4\pi z(x)/\lambda]dx & \text{reflection} \\ T_0\int \exp[-i2\pi(n_{TCO}-1)z(x)/\lambda]dx & \text{transmission} \end{cases}. \tag{A8}$$

The reflectance or transmittance can then be defined as: I^{sc}/I^{total}. So, the coherent parts of the reflection and transmission of random rough surfaces can be written as follows:

$$R_c = R_0\left|\int_{-\infty}^{\infty} D(z)e^{-4\pi iz/\lambda}dz\right|^2, \tag{A9}$$

$$T_c = T_0\left|\int_{-\infty}^{\infty} D(z)e^{-2\pi iz/\lambda(n-1)}dz\right|^2, \tag{A10}$$

where the R_c and T_c are the coherent reflectance and transmittance, and D(z) is the aforementioned density function of surface height distribution. Under normal incidence conditions and specular observation, the angle of incidence, and the refraction/reflection angle are both zero.

Another way of understanding the similarity of coherent reflection and transmission coefficient can be found in Porteus's paper.[8] As shown in the paper, the scattered electromagnetic field can be expressed as:

$$\langle|E^{sc}|^2\rangle = |C|^2k^2\int D(z)D(z')e^{-i\vec{k}\cdot(\vec{r}-\vec{r}')}dxdydzdx'dy'dz', \tag{A11}$$

where $\vec{k}=\vec{k}_d-\vec{k}_i$ (i.e., the difference between incident and diffracted wave number). This is because, in the non-multiple

scattering case, the difference between transmission and the reflection wave is only at the phase change we pointed out earlier. The difference between reflection and transmission coefficient should be $4\pi/\lambda$ and $2(n_{TCO}-1)\ \pi/\lambda$.

[1]P. Campbell and M. A. Green, J. Appl. Phys. **62**, 243 (1987).
[2]M. Kambe, A. Takahashi, N. Taneda, K. Masumo, T. Oyama, and K. Sato, 33rd IEEE Photovoltaic Specialists Conference, San Diego, CA, 11–16 May 2008, pp. 1–4.
[3]N.-N. Feng, J. Michel, L. Zeng, J. Liu, C.-Y. Hong, L. C. Kimerling, and X. Duan, IEEE Trans. Electron Devices **54**, 1926 (2007).
[4]A. Hongsingthong, T. Krajangsang, I. A. Yunaz, S. Miyajima, and M. Konagai, Appl. Phys. Express **3**, 051102 (2010).
[5]J. Krc, B. Lipovsek, M. Bokalic, A. Campa, T. Oyama, M. Kambe, T. Matsui, H. Sai, M. Kondo, and M. Topi, Thin Solid Films **518**, 3054 (2010).
[6]G. Yue, L. Sivec, J. M. Owens, B. Yan, J. Yang, and S. Guha, Appl. Phys. Lett. **95**, 263501 (2009).
[7]H. Davies, Proc. IEEE **101**, 209 (1954).
[8]J. O. Porteus, J. Opt. Soc. Am. **53**, 1394 (1963).
[9]P. Beckmann and A. Spizzichino, *The Scattering of Electromagnetic Waves from Rough Surfaces* (Pergamon, Oxford, 1963).
[10]K. Jaeger and M. Zeman, *Optics for Solar Energy, OSA Technical Digest* (Optical Society of America, New York, 2010).
[11]D. Dominé, F.-J. Haug, C. Battaglia, and C. Ballif, J. Appl. Phys. **107**, 044504 (2010).
[12]M. Zeman, R. A. C. M. M. van Swaaij, J. W. Metselaar, and R. E. I. Schropp, J. Appl. Phys. **88**, 6436 (2000).
[13]I. Simonsen, A. Larsen, E. Andreassen, E. Ommundsen, and K. Nord-Varhaug, Phys. Rev. A **79**, 063813 (2009).
[14]H. Ragheba and E. R. Hancock, Pattern Recogn. **40**, 2004 (2007).
[15]E. Marx and T. V. Vorburger, Appl. Opt. **29**, 3613 (1990).
[16]J. Caron, J. Lafait, and C. Andraud, Opt. Commun. **207**, 17 (2002).
[17]J. A. Sánchez-Gil and M. Nieto-Vesperinas, J. Opt. Soc. Am. A **8**, 1270 (1991).
[18]P. B. Nagy and L. Adler, J. Acoust. Soc. Am. **82**, 193 (1987).
[19]H. P. Pillai, J. Krc, and M. Zeman, Proceedings of Semiconductor Advances for Future Electronics, Veldhoven, The Netherlands, 28–30 November 2001, pp.159–162.
[20]D. Dominé, P. Buehlmann, J. Bailat, A. Billet, A. Feltrin, and C. Ballif, Phys. Status Solidi (RRL) **2**, 163 (2008).
[21]N. Taneda, K. MASUMO, M. Kambe, T. Oyama, and K. Sato, 23rd European Photovoltaic Solar Energy Conference, Valencia, Spain, 1–5 September 2008, pp. 2084–2087.
[22]C. Cording, International Workshop on Glass for Harvesting, Storage and Efficient usage of Solar Energy, Pittsburgh, PA, 16–18 November 2008, Technical Session II.
[23]J. Krc, M. Zeman, O. Kluth, F. Smole, and M. Topic, Thin Solid Films **426**, 296 (2003).
[24]J. Krč, M. Zeman, O. Kluth, F. Smole, and M. Topic, J. Appl. Phys. **92**, 749 (2002).
[25]H. E. Bennett, J. Opt. Soc. Am. **53**, 1389 (1963).
[26]M. Nieto-Vesperinas, J. A. Sánchez-Gil, A. J. Sant, and J. C. Dainty, Opt. Lett. **15**, 1261 (1990).
[27]A. E. Rakhshani, Y. Makdisi, and H. A. Ramazaniyan, J. Appl. Phys. **83**, 1049 (1998).
[28]J. M. Bennett and L. Mattsson, *Introduction to Surface Roughness and Scattering* (Optical Society of America, Washington, DC, 1989), Chap. 5, pp. 57–68.
[29]J. M. Soto-Crespo and M. Nieto-Vesperinas, J. Opt. Soc. Am. A **6**, 367 (1989).
[30]E. I. Thorsos, J. Acoust. Soc. Am. **83**, 78 (1988).
[31]M. Nieto-Vesperinas, *Scattering and Diffraction in Physical Optics* (Wiley, New York, 1991), Chap. 7.